

RESEARCH ARTICLE

10.1002/2016MS000678

Key Points:

- Precipitation forecasting investigated in river basins affected by monsoon-driven floods
- Sensitivity of parameterization schemes and scales studied for downscaling of global Numerical Weather Prediction (NWP) model-based forecasts
- The likely best combination identified using Ganges-Brahmaputra basins and validated over the Indus basin
- A common set of parameterization configuration and scale could further advance operational forecasting of precipitation

Correspondence to:

F. Hossain,
fhossain@uw.edu

Citation:

Sikder, S., and F. Hossain (2016), Assessment of the weather research and forecasting model generalized parameterization schemes for advancement of precipitation forecasting in monsoon-driven river basins, *J. Adv. Model. Earth Syst.*, 8, doi:10.1002/2016MS000678.

Received 27 MAR 2016

Accepted 5 JUL 2016

Accepted article online 11 JUL 2016

© 2016. The Authors.

This is an open access article under the terms of the Creative Commons Attribution-NonCommercial-NoDerivs License, which permits use and distribution in any medium, provided the original work is properly cited, the use is non-commercial and no modifications or adaptations are made.

Assessment of the weather research and forecasting model generalized parameterization schemes for advancement of precipitation forecasting in monsoon-driven river basins

Safat Sikder¹ and Faisal Hossain¹

¹Department of Civil and Environmental Engineering, University of Washington, Seattle, Washington, USA

Abstract Some of the world's largest and flood-prone river basins experience a seasonal flood regime driven by the monsoon weather system. Highly populated river basins with extensive rain-fed agricultural productivity such as the Ganges, Indus, Brahmaputra, Irrawaddy, and Mekong are examples of monsoon-driven river basins. It is therefore appropriate to investigate how precipitation forecasts from numerical models can advance flood forecasting in these basins. In this study, the Weather Research and Forecasting model was used to evaluate downscaling of coarse-resolution global precipitation forecasts from a numerical weather prediction model. Sensitivity studies were conducted using the TOPSIS analysis to identify the likely best set of microphysics and cumulus parameterization schemes, and spatial resolution from a total set of 15 combinations. This identified best set can pinpoint specific parameterizations needing further development to advance flood forecasting in monsoon-dominated regimes. It was found that the Betts-Miller-Janjic cumulus parameterization scheme with WRF Single-Moment 5-class, WRF Single-Moment 6-class, and Thompson microphysics schemes exhibited the most skill in the Ganges-Brahmaputra-Meghna basins. Finer spatial resolution (3 km) without cumulus parameterization schemes did not yield significant improvements. The short-listed set of the likely best microphysics-cumulus parameterization configurations was found to also hold true for the Indus basin. The lesson learned from this study is that a common set of model parameterization and spatial resolution exists for monsoon-driven seasonal flood regimes at least in South Asian river basins.

1. Introduction

Perhaps the most challenging part of flood forecasting is the lack of meteorological observations, particularly precipitation [Liu *et al.*, 2012]. The problem is critical in the transboundary or international river basins where it is almost impossible to obtain reliable precipitation data from the upstream regions in near real-time due to hydropolitical issues [Hopson and Webster, 2010; Hossain *et al.*, 2007; Hossain and Katiyar, 2006]. A report by UN-Water [2008] shows that 40% of the global population resides in the 263 transboundary or International River basins. Moreover, if the real-time (i.e., nowcast) observed data (e.g., rain gauge data, satellite-observed precipitation) are available, these allow forecasting of floods limited by the time taken for runoff once generated in the river, to flow from the most upstream location to the downstream sink of an ocean or lake. In order to extend this forecast lead time beyond the maximum bounded by a basin's time of concentration, precipitation forecasts are needed. Thus, the use of model-based precipitation forecasts in flood forecasting has recently become a trend among many flood forecasting agencies and flood management communities [e.g., Jasper *et al.*, 2002; Verbunt *et al.*, 2006; Liguori *et al.*, 2012; Liu *et al.*, 2015]. For example, the Flood Forecasting and Warning Center of Bangladesh now takes advantage of 5 day precipitation forecasts in the Ganges-Brahmaputra basins to improve skill of its 5 day river level forecast product during the monsoon season [FFWC, 2014].

Precipitation forecasts using Numerical Weather Prediction (NWP) models still face difficulties at scales relevant for flood forecasting [e.g., Ebert, 2001; Nam *et al.*, 2014; Yucl *et al.*, 2015]. For example, for convective precipitation processes, this is more challenging due to the lack of better representation of convective processes through appropriate parameterizations [Lowrey and Yang, 2008; Yucl and Onen, 2014]. Therefore, investigations are required to understand the physical properties of small scale meteorological processes. Assessment of the small-scale meteorological processes (e.g., thunderstorm) can be performed by finer

scale NWP models. Many studies suggest that higher spatial resolution models perform better when the precipitation is intense [e.g., Roberts *et al.*, 2009; Givati *et al.*, 2012; Jang and Hong, 2014]. Due to the computational limitations of global modeling, most global NWP model-based precipitation forecasts are available at large spatial scales. For example, the Global Forecast System (GFS) of the National Oceanic and Atmospheric Administration (NOAA) produces nowcast and 10 day forecasts of meteorological conditions and precipitation at 0.25° resolution every 6 h. Naturally, there is therefore a need to explore downscaling options available with finer resolution numerical models such as the Weather, Research and Forecasting (WRF) model [Skamarock *et al.*, 2008]. A recent study by Kumar *et al.* [2016] showed that the quality of global NWP model-forecasted precipitation over the Indian continent can be improved by downscaling using the WRF.

In many cases, it is not computationally feasible to operate a regional numerical weather prediction model (e.g., WRF) routinely using a very fine resolution grid over a large domain for flood forecasting operations. For such issues, subgrid-scale parameterization schemes, nesting, and data assimilation techniques have been introduced in numerical models to improve downscaled output. Thus, the simulated precipitation can be sensitive to spatial resolution, parameterization schemes, nesting ratios, and domain size of the model. Many studies evaluated the sensitivity of these features. Liu *et al.* [2012] studied the downscaling ratio between the nests in the modeling domain. They showed that the performance of the model to predict precipitation decreased with high downscaling ratios (e.g., 1:10). In addition, they noted that model performance is also sensitive to domain size. Model parameterization schemes are likely the most studied feature to optimize model performance. For example, Efsthioiu *et al.* [2013] evaluated WRF model performance for a heavy precipitation event in northern Greece using different planetary boundary layer options and microphysics schemes. Mannan *et al.* [2013] tested the WRF model using different microphysics for an intense rainfall event in Bangladesh. Rao *et al.* [2007] assessed the model for several Indian heavy precipitation events using different microphysics and cumulus parameterization schemes. Pennelly *et al.* [2014] evaluated five different cumulus parameterization schemes for heavy rainfall in Alberta with different grid spacing and reported that at 6 km resolution or higher, the model performance is independent of cumulus physics parameterization schemes.

Another critical issue of downscaling forecasted precipitation from global NWP models is the skill dependence on forecast lead time. Usually, precipitation forecast deteriorates with increasing lead time [Georgakakos *et al.*, 2014]. Accuracy of the forecasted precipitation also depends on the model parameterization and spatial resolution. Therefore, evaluation of different sets of parameterization schemes and spatial resolution as a function of precipitation estimation accuracy and forecast lead time is important for advancing numerical model-based downscaling of global NWP forecasts for operational flood forecasting. Such an evaluation can pinpoint a more manageable set of parameterizations that may need further refinement through atmospheric field studies before operationalization in flood forecasting applications.

In this study, we investigate the performance of the WRF model to predict (nowcast and forecast) precipitation for monsoon-affected flood-prone river basins. We apply a numerical model (e.g., WRF) for spatial downscaling of global NWP model output on precipitation for flood forecasting applications. The definition of monsoon weather systems and its spatial domain as outlined by Ramage [1971] was used and is shown in Figure 1. This monsoon boundary covers almost 20% of the world's surface, and incorporates some of the largest and most populous transboundary river basins (e.g., Ganges, Brahmaputra, Indus, Mekong, Salween, Upper Nile). The prevalence of transboundary flooding in such monsoon regions is critical as it negatively impacts downstream nations due to the lack of shared hydrometeorological observations in near real-time [Hossain and Katiyar, 2006].

This study explores the sensitivity of WRF physics parameterizations and spatial scale to identify a more optimal configuration for downscaling global NWP forecasts that is more likely to “work” in monsoon-dominated regions. The goal is to derive a configuration that is computationally efficient and yet skillful enough for a large international river basin for eventual use in operational applications. The question we try to answer in this study is as follows: *Is it possible to identify the likely best set of parameterization schemes for cloud and cumulus processes and spatial resolution for WRF downscaling of global NWP forecasts that will hold true for most monsoon-affected river basins?* As mentioned earlier, such a set can make further refinement of model parameterizations (or proposal of new ones) through targeted field campaigns practically feasible due to a smaller working sample.

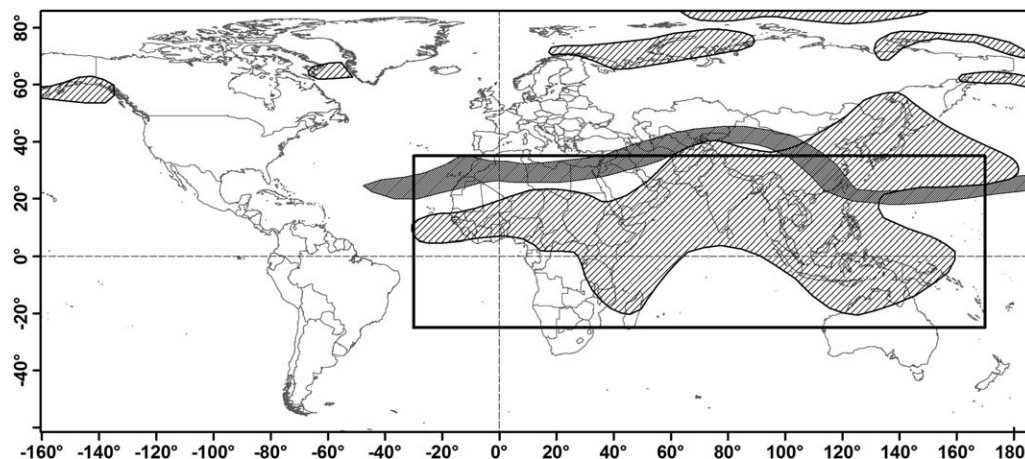


Figure 1. The area inside the box is the Monsoon climate regime, according to *Ramage* [1971]. The monsoonal areas defined by *Khromov* [1957] are shown by the hatched polygon [after *Ramage*, 1971].

2. Numerical Models for Precipitation Forecasting

The GFS is a global-scale NWP model developed by the NOAA. The model is run four times per day by the US National Weather Service to generate detailed and global output of atmospheric variables. At each run, the model generates a forecast up to 16 days. The model simulation is divided into two steps. In the first step, the GFS generates forecast every 3 h from 000 to 240 h (i.e., 10 days). In the next step, the model generates forecast every 12 h from 240 to 384 h (i.e., next 6 days). The model resolution is different in both steps. However, the 16 day forecast data are available at 0.25°, 0.5°, 1°, and 2.5° resolution through the National Center for Environmental Prediction (NCEP). NCEP uses the same GFS model to run with more observational data and generate a more accurate daily output. The product is known as NCEP final analysis. The NCEP final analysis (FNL from GFS) data are available at 1° resolution every 6 h.

In this study, we used the WRF-ARW V3.7.1 to dynamically downscale the global NWP model outputs. The WRF is a new generation numerical weather prediction model with advanced dynamics, physics, and numerical schemes, and was developed from its predecessor, the MM5 model. It is a mesoscale meteorological model that uses fully compressible, nonhydrostatic Euler equations. For horizontal discretization, it uses Arakawa-C grid staggering and a third-order Runge-Kutta integration scheme for time separation. The model is capable of dealing with both one-way and two-way nesting. Details of the dynamics and physics of the WRF model are described in *Skamarock et al.* [2008].

In a numerical model like WRF, the Microphysics (MP) and Cumulus Parameterization (CP) schemes are mainly responsible for precipitation generation. Water vapor, cloud, and precipitation process are explicitly resolved by the microphysics. The subgrid-scale convective process and shallow clouds are managed by the cumulus parameterization. The Indian summer monsoon rainfall prediction using the WRF model has been found to be sensitive to the choice of convective parameterization scheme [*Srinivas et al.*, 2015]. Many studies on the Indian summer monsoon rainfall reported that the Betts-Miller-Janjic CP scheme performs better in that region [e.g., *Mukhopadhyay et al.*, 2010; *Kumar et al.*, 2010; *Vaidya*, 2006; *Srinivas et al.*, 2013].

The cloud microphysics scheme is mainly responsible for nonconvective rainfall in the coarse resolution (>10 km) WRF model. *Rajeevan et al.* [2010] conducted a sensitivity test of four different WRF microphysics schemes on a severe thunderstorm over southeast India. They found that the Thompson scheme performed well out of the four microphysics options, although the Morrison scheme was the most sophisticated among them. At high spatial resolution (less than 5 km), numerical models are expected to capture the convective processes and therefore the use of a convective scheme is optional [*Hsiao et al.*, 2013]. Thus, the sensitivity of different microphysics schemes over the Indian monsoon rainfall needs to be evaluated, particularly for very high-resolution models (<10 km). More recently, *Zheng et al.* [2016] identified that cloud microphysics alone was not sufficient to resolve convective processes at higher resolution in the WRF model. They compared high-resolution model simulations (grid increments of 9 km and 3 km) over the U.S.

Table 1. Selected MP-CP Parameterization Schemes for Evaluation Along With Other Parameterization Schemes

Physics Options	Parameterization Schemes
Microphysics (MP)	WRF Single Moment 3 Class Scheme (WSM3) [Hong et al., 2004] WRF Single Moment 5 Class Scheme (WSM5) [Hong et al., 2004] WRF Single Moment 6 Class Scheme (WSM6) [Hong and Lim, 2006] Thompson Scheme (TS) [Thompson et al., 2008] Morrison 2-Moment Scheme (MDM) [Morrison and Thompson, 2009]
Cumulus Parameterization (CP)	Kain-Fritsch Scheme (KF) [Kain, 2004] Betts-Miller-Janjic Scheme (BMJ) [Janjic, 1994] Grell-Freitas Ensemble Scheme (GF) [Grell and Freitas, 2014]
Planetary Boundary Layer (PBL)	Yonsei University Scheme (YSU) [Hong et al., 2006]
Radiation-Shortwave (Ra-SW)	Dudhia Shortwave Scheme [Dudhia, 1989]
Radiation-Longwave (Ra-LW)	RRTM Longwave Scheme [Mlawer et al., 1997]
Land Surface (SF_SURFACE)	Unified Noah Land Surface Model [Tewari et al., 2004]
Surface Layer (SF_SFCLAY)	MM5 Similarity Scheme [Zhang and Anthes, 1982]

southern Great Plains with no convective scheme runs, and reported that the updated Kain–Fritsch schemes showed better result in both resolutions.

Precipitation is also sensitive to the planetary boundary layer (PBL). *Ulate et al.* [2014] studied the sensitivity of CP-PBL parameterization schemes for the Indian Ocean and Maritime Continent water cycle, and reported that the water cycle was more sensitive to the PBL than CP. However, a dry bias was found with the Mellor-Yamada-Janjic PBL scheme, while the Yonsei University Scheme performed relatively better. A similar observation was reported by *Efstathiou et al.* [2013] for the heavy rain rate over the eastern Chalkidiki peninsula in northern Greece. Therefore, the Yonsei University PBL scheme was used in this study. Table 1 provides the list of microphysics and cumulus parameterization schemes along with other parameterization schemes used in this study.

3. Study Approach and Methodology

The main objective of this study is to identify the likely best set of parameterization schemes and spatial resolution that can hold true for most river basins in monsoon-driven flood-prone regions. Due to the computationally prohibitive nature of running WRF, a 1 month period during the monsoon season was selected. This period had short dry spells that allowed for assessment of false rain simulation. We selected the monsoon-driven Ganges-Brahmaputra-Meghna (GBM) basins as the test river basin to explore the various combinations of parameterization and scale (Figure 2). GBM basins have the characteristic of incorporating three river basins of contrasting size, precipitation intensity, times of concentration, and flood regime [Mirza et al., 1998]. Here, Meghna is the smallest in size and response time while Ganges is the largest. Brahmaputra has steep terrain with high flow rate flood regime, often exceeding 70,000 m³/s during the Monsoon season.

We set up the WRF model for the entire GBM river basin system (Figure 2). The model setup consisted of three one-way nested domains, where the smallest-scale domain was divided further into two subdomains (D03 and D04) for computational efficiency (Figure 2). The smallest domains span different climatic regions of the GBM basin, where there is strong variability in precipitation climatology. Domain 3 covers the heavy rainy region which is a mainly humid subtropical zone and Domain 4 covers the semiarid area (less rainy) of Western India. The outermost domain (D01) has 27 km grid resolution and covers the entire Indian subcontinent, northern Indian Ocean, southern part of central Asia, northern part of Southeast Asia, and a part of China (spanning 54°E–106°E and 2°N–40°N). The smallest domains (i.e., D03 and D04) have grids with 3 km resolution. Domains 3 and 4 were configured without any CP parameterization, assuming that the MP is capable of explicitly solving the convective process in 3 km resolution. The second domain (D02) is the child of the outermost domain (D01) and parent of the smallest domains (D03 and D04). The default two-way nesting in WRF updates the parent domain using the results of the child domain. Here, we used one-way nesting to keep the parent domain output “as is” for further analysis. A 1 month time period of the Indian summer monsoon from 5 August 2015 to 4 September 2015 was chosen as the simulation period. During this period several heavy rainfall events occurred in the region. The simulation time step of the outer

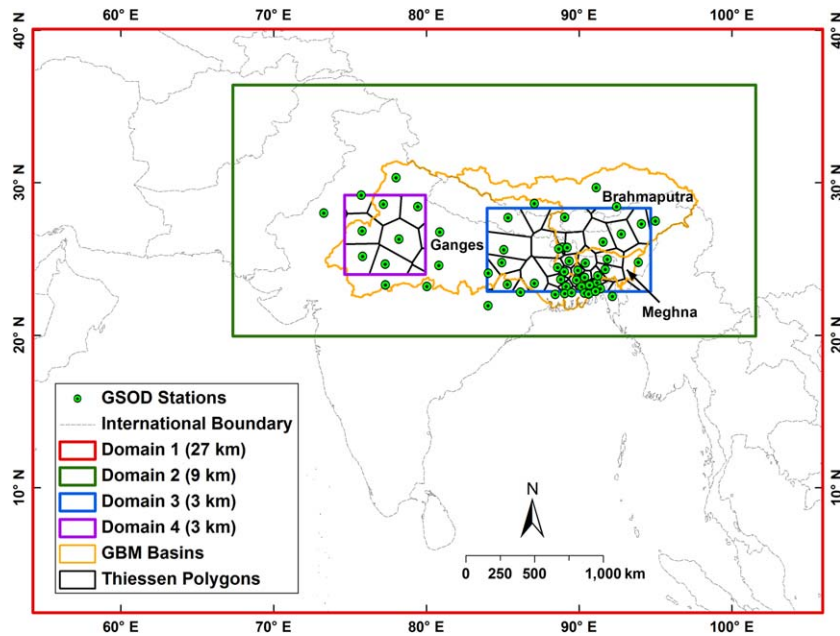


Figure 2. WRF model domains for the GBM basin. Here, Domain 3 and 4 are for the heavy rainy and less rainy areas, respectively. The weather stations (obtained from NCDC Global Summary of the Day-GSOD) are shown along with the Thiessen polygons inside the 3 km domains. Data from these stations were used to calculate the areal-averaged observed precipitation.

domain (i.e., D01) was selected as 90 s. Model outputs were saved every 3 h, although output of every 24 h interval was used.

To test if the likely best configuration of parameterizations identified for GBM basins is applicable to other regions, a similar WRF setup was prepared for the Indus river basin (Figure 3) with two one-way nested domains. The outermost domain (D01) has 27 km resolution and innermost domain (D02) has 9 km resolution. The analysis extent (Figure 3) covers almost entire Indus river basin. The outer domain covers nearly

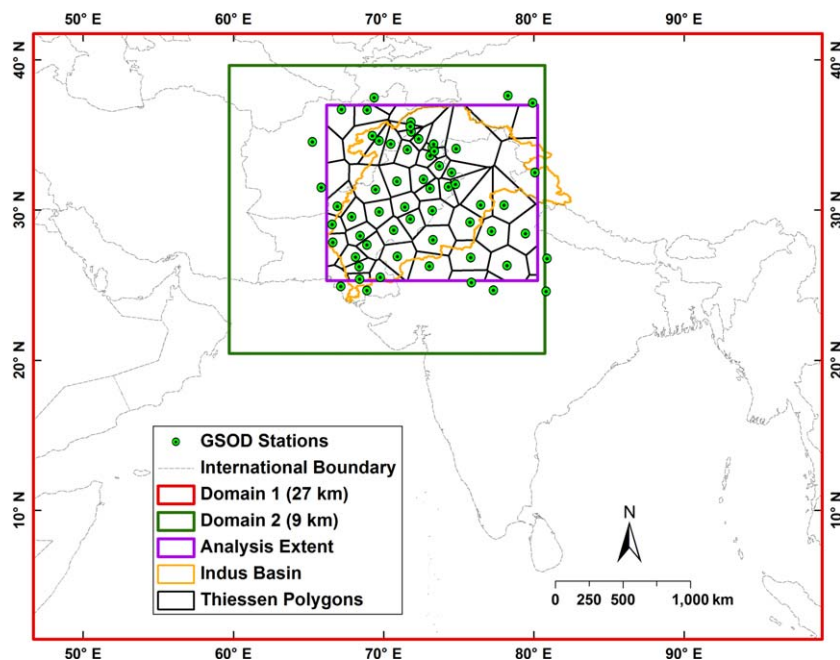


Figure 3. Same as Figure 2 but for the Indus basin to test if the likely best configuration identified using GBM basins hold true for Indus. Here, the GSOD stations and their respective Thiessen polygons are shown over the entire domain of analysis.

the same area as domain 1 of the GBM basin (47°N–99°N and 2°N–42°N). Given limitations of CPU resources, a one week time period (25–31 July 2010) was selected for testing the efficacy of GBM-derived configuration. We consider this an appropriate period as it includes a severe flood event with basin-wide precipitation peaking on 29 July 2010 and leading to large-scale floods in most parts of Pakistan. All other parameters and model configurations remained the same.

As seen from Table 1, five MP schemes and three CP schemes were chosen at three different spatial resolutions (27, 9, and 3 km) to evaluate the sensitivity to precipitation simulations. Parameterization schemes beyond CP and MP were selected based on compatibility with the monsoon-driven climate [e.g., *Ahasan and Khan*, 2013; *Kumar et al.*, 2012; *Rao et al.*, 2007] and are also shown in Table 1. However, these parameterizations were not part of the sensitivity study. A total of 15 MP-CP combinations (5 MP \times 3 CP) were evaluated in GBM basins over a one month time period to identify the existence of the likely best MP-CP combination and spatial scale. Each combination is denoted hereafter by their MP-CP abbreviation shown in Table 1. For example, WSM5-KF means the combination of the WRF Single Moment 5 class microphysics and Kain-Fritsch cumulus parameterization. The 6 hourly 1° resolution NCEP GFS final analysis data were used as the boundary data and initial condition for a continuous 1 month simulation of the GBM basins. From the sensitivity study, the three best MP-CP combinations and spatial scales were chosen according to their performance in simulating precipitation in nowcast mode. Thereafter, we applied these MP-CP combinations and spatial resolution to the Indus river basin. The initial and boundary data source remained the same as in the GBM nowcast mode for the Indus river basin. For assessment of the MP-CP combination in the forecast mode, two storm events in the GBM basin were selected and simulated using the GFS forecast data as the model boundary up to 10 days lead time. To generate the forecast for 10 different lead times of a storm event, a total of 10 simulations were carried out for a particular MP-CP combination, starting 10 days before the storm event followed by 9 days, 8 days and so on. The 3 hourly 0.5° resolution GFS forecast data were used as the boundary condition for the forecast simulation, while the initial condition of each simulation was taken from the previous day's model output. For example, initial conditions for the 9 day lead simulation (i.e., starting 9 days before the storm event) were taken from the 1st date output of the 10 day lead simulation thereby minimizing the effect of the model spin-up time error to generate more accurate output at smaller lead times.

4. Data

In our parameterization and spatial resolution sensitivity experiments, the 6 hourly 1° \times 1° resolution NCEP GFS final analyses data were used as the boundary in the WRF model [e.g., *Rao et al.*, 2007]. These boundary data were available through the University Cooperation for Atmospheric Research-Research Data Archive (<http://rda.ucar.edu/datasets/ds083.2/>). Data from the same source were used as the boundary to evaluate the performance of the likely best MP-CP combinations over the Indus basin for the July 2010 storm event. To evaluate the performance of the MP-CP schemes in forecast mode with different lead times, forecasted boundary data were used. In the case of a forecasted boundary, we used 3 hourly 0.5° \times 0.5° resolution archived GFS forecast up to 10 days (<http://www.nco.ncep.noaa.gov/pmb/products/gfs/>).

Simulated precipitation was compared against satellite-estimated precipitation from the Global Precipitation Measurement (GPM)-Integrated Multi-satellite Retrievals for GPM (IMERG) final run data (30 min precipitation with 0.1° resolution). This global precipitation data set was prepared using satellite-estimated precipitation (from microwave and microwave-calibrated infrared), precipitation gauges analysis [*Huffman et al.*, 2015]. GPM is the core satellite of this data set. WRF-simulated precipitation over the Indus basin precipitation is compared against the daily 0.25° \times 0.25° Climate Hazards Group InfraRed Precipitation with Station data-CHIRPS [*Funk et al.*, 2015], as GPM-IMERG data record begins from 2014. This historical data set (since 1981) was prepared using satellite imagery and gauged station data. The mean daily precipitation of CHIRPS data shows consistency with GPM-IMERG over the GBM basin for peak one month of the 2015 monsoon (Figure 4). Therefore, the comparison between the simulated precipitation performance of GBM basin (with respect to GPM-IMERG) and Indus basin (with respect to CHIRPS) is fair. Finally, the amount of predicted precipitation (areal-averaged precipitation) was evaluated against in situ ground station data available from the World Meteorological Organization through NCDC (National Climatic Data Center) GSOD (Global Surface Summary of the Day). The heavy rainy area of the GBM basin (D03) covers 43 GSOD stations

while the less rainy area of the GBM basin (D04) covers 13. Sixty GSOD stations located in the Indus basin were used and the point precipitation values were converted to areal averages using the Thiessen polygon method (see Figures 2 and 3).

5. Performance Criteria

We used error metrics proposed by *Liu et al.* [2012] to evaluate model output performance with respect to observed data. Four categorical metrics were used. These included probability of detection (POD), the frequency bias index (FBI), the false alarm ratio (FAR), and critical success index (CSI). The POD indicates the probability of detection of rainfall, while FAR is the probability of the false rain (alarm) produced by the simulation. The CSI also indicates the probability of the detection, but with respect to the total rainfall predicted by model and observation. The FBI evaluates the tendency to over or underestimate simulated rainfall with respect to observed data. The ideal scores for POD, FBI, FAR, and CSI are 1, 1, 0, and 1, respectively. Three continuous metrics, including the root mean square error (RMSE), the mean bias error (MBE), and the standard deviation (SD) were used in this study. Both RMSE and SD indicate the amount of error in predicted precipitation without showing the bias. The MBE shows the bias of the simulated precipitation with respect to the observed.

The categorical metrics were calculated with respect to the gridded satellite final (gauge-calibrated) products (i.e., GPM-IMERG for GBM and CHIRPS for Indus), while the other three error metrics were calculated with respect to the areal-averaged observed precipitation determined from NCDC-GSOD station data. Here, each error metric represents different characteristics of the performance of simulated precipitation. It is difficult to choose the best options based on these seven different error metrics. Therefore, a multicriteria decision analysis was carried out to find the likely best MP-CP combination over the GBM basin. Furthermore, two unified performance scores were used to compare the results from different model configurations. The description of the multicriteria decision analysis technique and the unified performance scores are given in the next sections.

5.1. Multicriteria Decision Analysis

We used a multicriteria decision analysis technique named TOPSIS (Technique for Order of Preference by Similarity to Ideal Solution) to find the likely best MP-CP combinations. TOPSIS was first developed by *Hwang and Yoon* [1981] and later modified and used in numerous studies [e.g., *Milani et al.*, 2005; *Upadhyaya and Ramsankaran*, 2014]. This multicriteria decision analysis technique determines the best alternative using the shortest and longest geometric distance from the positive and negative ideal solution, respectively [*Assari et al.*, 2012].

TOPSIS consists of six steps, starting with a decision matrix with different alternatives and criteria. In this study, we used 15 different MP-CP combinations to find the likely best combination for monsoon-driven weather. These 15 MP-CP combinations along with three different spatial resolutions provided 45 different alternatives in this case. Therefore, the decision matrix in this study had 45 alternatives and 7 criteria (i.e., 4 categorical and 3 continuous error metrics). The value of each criterion indicates the performance of different alternatives. In TOPSIS, each criterion should have the evaluation as “more is better” or “less is better.” To meet the requirements, the FBI and MBE were rescaled. Both rescaled metrics were ranging from 0 to ∞ , where 0 is the perfect score. Therefore, the POD and CSI are “more is better” and FAR, rescaled FBI, RMSE, SD, and rescaled MBE are “less is better” criteria in this study. We used equal weight for all criteria. Finally, the relative closeness to the ideal solution was computed. Hereafter, this computed value is denoted as TOPSIS RCV (Relative Closeness Value). The higher TOPSIS RCV means closer to the observed data or more accurate alternative.

5.2. Unified Performance Scores

The TOPSIS RCV is a relative value to identify the best alternative based on the given criteria. Which means that the value is not absolute and may change with different sets of alternatives. Therefore, two unified performance scores were used to compare overall model performance across different configurations, where the score of each alternative is not relative to others. At first, the values of all error metrics were rescaled to calculate the performance scores.

Table 2. Relationship Between Original and Rescaled Error Metrics^a

Rescaled Error Metrics	Threshold Value
POD _r = POD	N/A
If FBI > 1: FBI _r = (2-FBI)	+2 max
If FBI <= 1: FBI _r = FBI	
FAR _r = 1-FAR	N/A
CSI _r = CSI	N/A
If MBE > 0: MBE _r = MBE/6	-6 to +6
If MBE < 0: MBE _r = MBE/-6	
RMSE _r = (1-RMSE/12)	+12 max
SD _r = (1-SD/12)	+12 max

^aValues of the rescaled error metrics range from 0 to 1, and were used to calculate the “Unified Score” and “Spatial Extent Score.”

Table 2 shows the relationship between the original error metric and rescaled metric (where subscript “r” denotes “rescaled”). Here, the thresholds were selected based on the highest and lowest metric values. All rescaled values range from 0 to 1, where 0 represents the worst case and 1 is for an ideal case. Thereafter, a unified score was calculated by assigning equal weights to all rescaled error metrics (i.e., by averaging all rescaled values). The point of deriving a unified score was to allow a convenient and multidimensional assessment of precipita-

tion simulation quality for various WRF configurations. Here, a higher unified score means better model performance or closer to the observed data.

$$Unified\ Score = \left(\frac{POD_r + FBI_r + FAR_r + CSI_r + MBE_r + RMSE_r + SD_r}{7} \right) \quad (1)$$

Another performance score was calculated to evaluate model performance in forecast mode using only the rescaled categorical metrics denoted here as the spatial extent score. Like the unified score, the spatial extent score ranges from 0 to 1 with 1 being the ideal value. This score shows the overall model performance in terms of spatial distribution of precipitation.

$$Spatial\ Extent\ Score = \left(\frac{POD_r + FBI_r + FAR_r + CSI_r}{4} \right) \quad (2)$$

6. Results and Discussion

6.1. Identifying the Likely Best Set of MP-CP Configurations

The model was simulated for 31 days over the GBM domain in nowcast mode to identify the likely best MP-CP combinations. Figure 4 shows a sample comparison between the mean daily precipitations of the study area from two MP-CP combinations with 9 km resolution (i.e., domain 2) and GPM-IMERG. The black boxes in Figure 4 are the analysis extent for heavy rainy areas and less rainy areas, and are equivalent to the area of Domains 3 and 4 of the GBM setup (Figure 2), respectively.

Figure 5 shows a sample comparison between the areal-averaged precipitation from two MP-CP combinations with 9 km resolution and NCDC-GSOD. For the combined case, both heavy rainy areas and less rainy areas were considered.

The spatial distribution of simulated precipitation was assessed using categorical metrics (i.e., POD, FBI, FAR, and CSI), which were calculated against the GPM-IMERG data for the heavy rainy area, less rainy area, and for the combined area. Figure 6 shows the comparison between the performance of WRF-modeled nowcast precipitation against GPM-IMERG for different MP-CP combinations and spatial resolutions according to different categorical metrics.

In the heavy rainy area, the POD of the simulated precipitation is relatively better with the BMJ and GF CP schemes. The performance of the GF-CP scheme is marginally better than BMJ in the humid subtropical zone (Figure 6a). In the less rainy or semiarid zone, performance of the BMJ scheme is significantly superior to the other two CP schemes (Figure 6b). In the combined case (Figure 6c), the performance of the BMJ and GF are almost similar, except for a few cases where the GF shows better performance (e.g., WSM3-GF). Across all conditions, the KF CP scheme shows poor performance. An almost similar pattern is visible in CSI (Figures 6d–6f). Both POD and CSI indicate that the BMJ and GF are adequate to detect rainfall. However, the GF exhibits better rain detection performance over wet regions (Figures 6a and 6d), while BMJ appears acceptable across all climatic conditions (Figures 6a, 6b, 6d, and 6e).

The FBI indicates that the BMJ and GF parameterization schemes have a tendency to overestimate precipitation, particularly when the resolution is coarse (Figures 6g–6i). In general, the KF scheme shows better

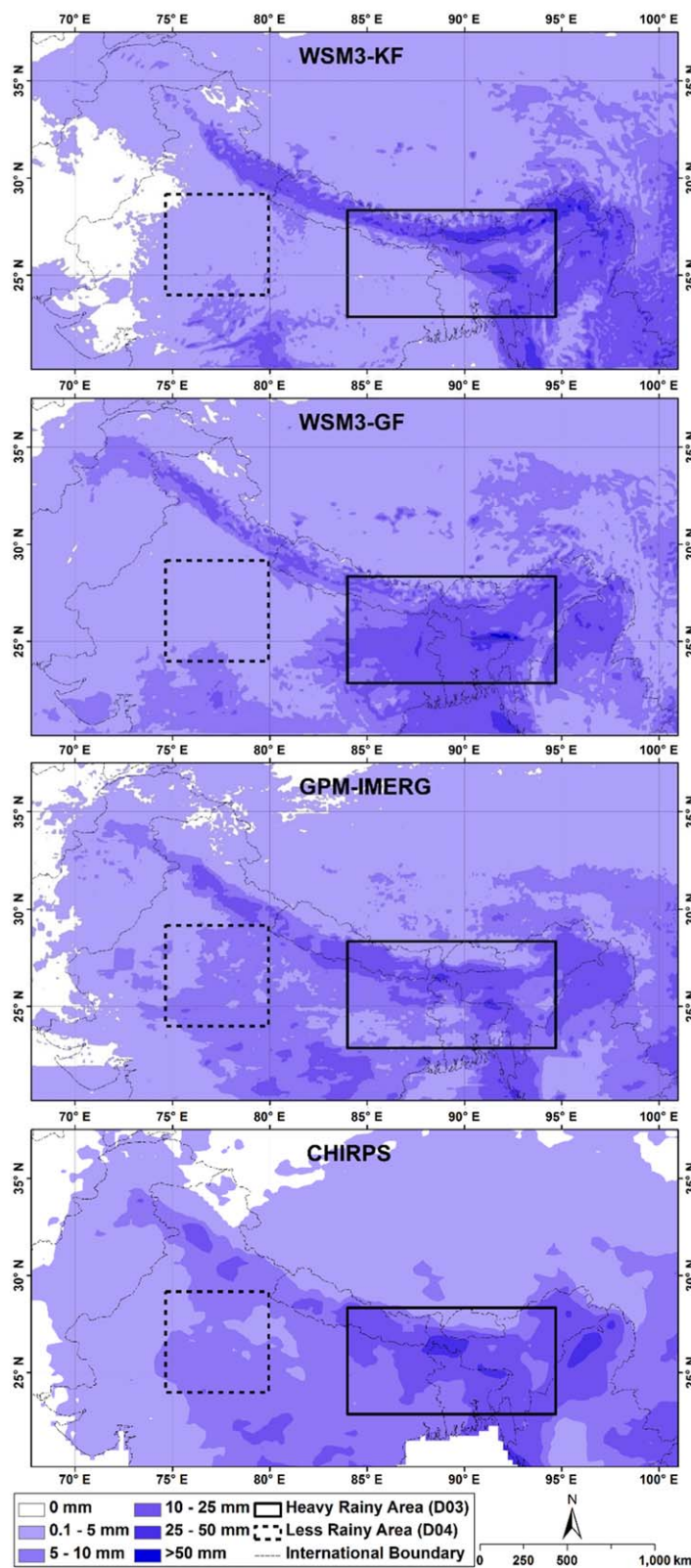


Figure 4. Mean daily precipitation (mm/day) from the WSM3-KF– 9 km simulation, WSM3-GF– 9 km simulation, GPM-IMERG (0.1° resolution), and CHIRPS (0.25° resolution) of the GBM basins for peak 1 month of the 2015 monsoon season. The boxes show the analysis extent of the heavy rainy area (same as Domain 3) and less rainy area (same as Domain 4).

performance (closer to 1) in coarse resolution (Figure 6i). The overall performance of the BMJ scheme is slightly better than the GF scheme in terms of FBI. One of the reasons of selecting continuous 1 month period in the monsoon including few dry spell was evaluating the false alarm of the simulated precipitation. However, the FAR in the heavy rainy area do not appear sensitive to a specific MP-CP combination (Figure 6j). This may be due to the fact that the wet region experiences rainfall almost every day and thus there is no opportunity for the WRF model to produce a false rain simulation. In the dry area, the performance of the GF scheme is noticeably poor in terms of FAR, while the KF scheme shows better results (Figure 6k). From Figure 6k, it is clear that the performance of the MDM MP scheme is worse than others and ultimately, it reduces the overall performance of the MDM MP scheme in combined conditions (Figure 6l). The above analysis of FAR reveals that the selection of the analysis area and period have an impact on the evaluation of model simulated precipitation performance. Similarly POD and CSI are not sensitive in case of dry period, when less or no rain occurs. Therefore, selection of multiple area with different characteristics and longer-time period is necessary to correctly evaluate the performance of simulated precipitation. From the analysis of the categorical metrics, we can see that the accuracy of simulating the spatial distribution of precipitation is quite sensitive to the CP schemes, and the overall performance of the BMJ scheme is better than the other two studied.

Daily areal-averaged precipitation for both simulated and

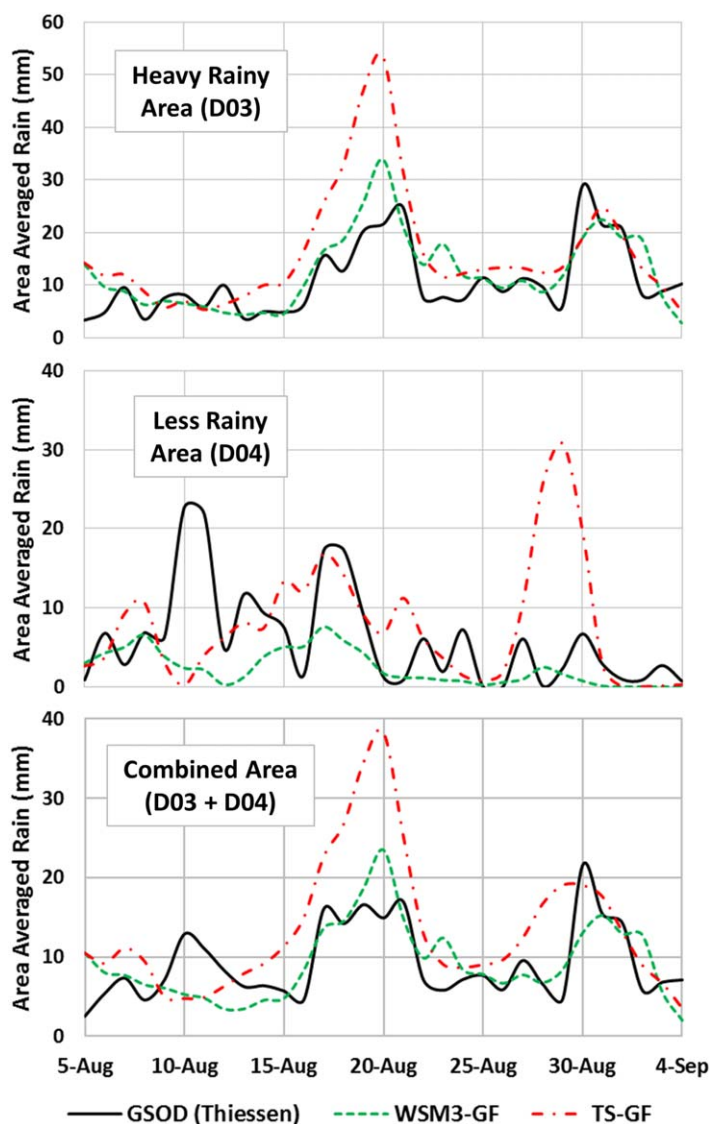


Figure 5. Areal-averaged precipitation from WSM3-GF– 9 km simulation, TS-GF– 9 km simulation, and GSOD station data (i.e., using the Thiessen polygon method). The areas covered in the analysis (i.e., D03, D04) are shown in Figure 4.

observed data were calculated to evaluate the metrics of MBE, RMSE, and SD. The NCDC-GSOD station data were used as reference Figure 7 depicts comparisons of the continuous error metrics or RMSE, SD, and MBE. From the MBE plot, it is clear that the WSM3 MP scheme has a tendency to yield negative bias (underestimation), while the GF-CP scheme has an opposite tendency of positive bias in all conditions (Figures 7a–7c). Patterns of the RMSE and SD are almost similar and show sensitivity of the CP schemes to the accuracy of the precipitation amount (Figures 7d–7i). The performance of the KF-CP scheme is worse for most cases of the wet climate region (Figures 7d and 7g). In dry conditions, the performance of the GF-CP scheme is relatively inferior to others (Figures 7e and 7h). In general, the BMJ scheme is better in all conditions in terms of areal-averaged precipitation.

Finally, the calculated TOPSIS RCV indicated that in wet area the BMJ and GF CP schemes perform relatively better than KF (Figure 8a). In the dry area, the BMJ is clearly superior (Figure 8b). Overall, performance of the BMJ is better in all conditions (Figure 8c). Similar results were found by other studies for the same region [e.g., Srinivas et al.,

2013; Kumar et al., 2010; Mukhopadhyay et al., 2010]. The MP schemes are not as sensitive as the CP schemes. The combination of the WSM3, WSM5, and WSM6 microphysics schemes with the BMJ cumulus parameterization scheme shows promising results in the GBM basins. The WSM3-GF with 27 and 9 km resolution and TF-GF, MDM-BMJ, MDM-GF with 3 km resolution also provide favorable results in combined cases. Considering the relatively poor performance of the GF-CP and MDM-MP scheme in the less rainy (semiarid) region and the difference between the TOPSIS RCV at different resolutions with the WSM3-GF, TF-GF, MDM-BMJ, MDM-GF combinations, we discarded combinations in further investigations (over Indus basin). Based on the sensitivity analyses shown in Figures 6–8, the likely best set of configurations selected for further investigation were: WSM5-BMJ, WSM6-BMJ, and TS-BMJ.

6.2. The Likely Ideal Spatial Resolution

In this study, we also evaluated the performance of three different spatial resolutions of the WRF model over the GBM basin domain. From the POD and CSI (Figures 6a–6f), it is clear that the probability of detecting precipitation is lower at finer resolutions (i.e., 3 km). Moreover, in most cases, the finer resolution model underestimates precipitation (Figures 6g–6i). In terms of FAR, the difference between the model resolutions

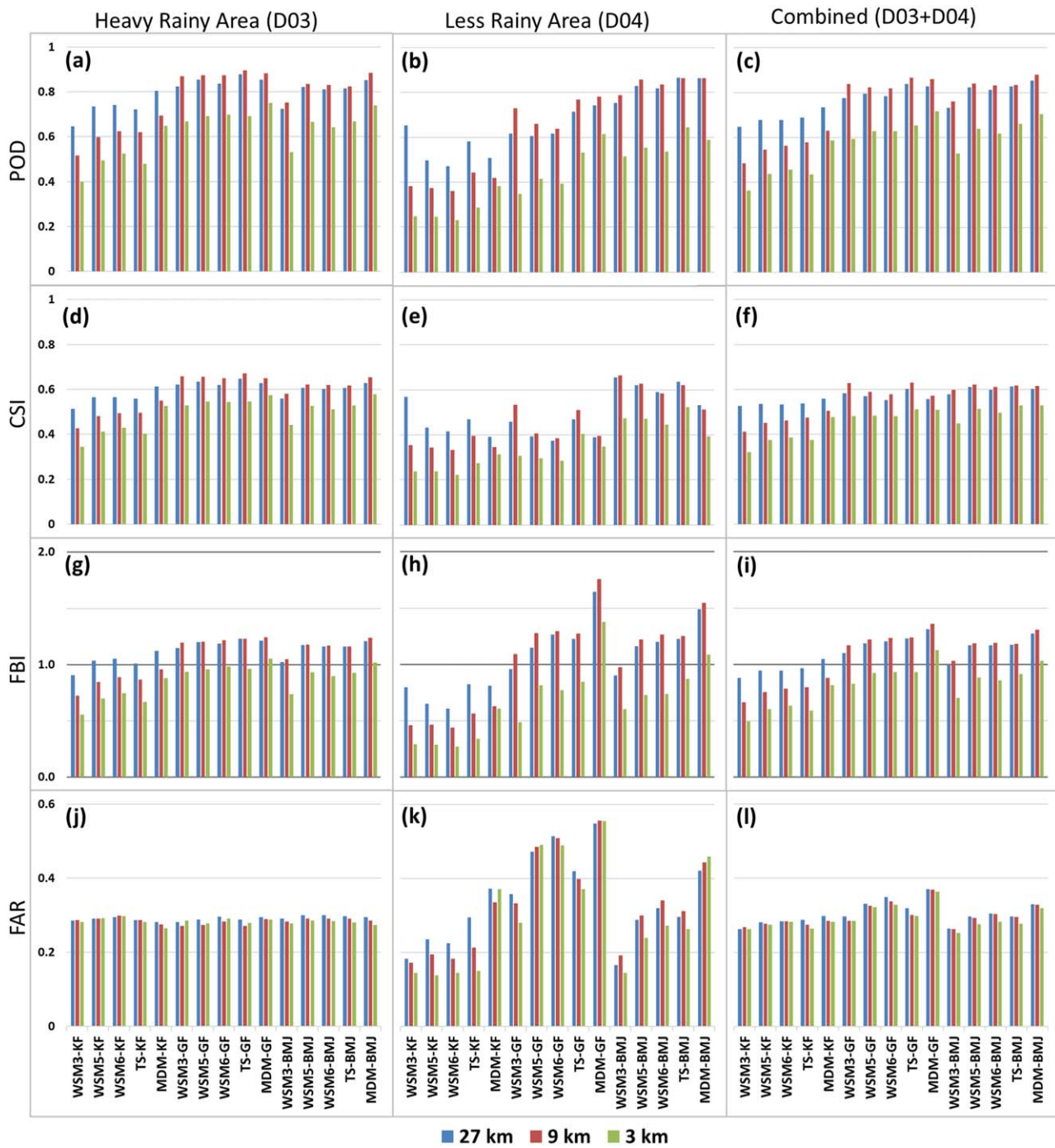


Figure 6. Comparison between different combinations of parameterizations (MP-CP and spatial resolution) in terms of spatial distribution accuracy in GBM basins for the 2015 monsoon season. Different spatial resolutions are represented by different lines in each subplot. In the case of POD, CSI, and FBI, the combination closer to 1 is more accurate, while for FAR, the value closer to 0 is better with respect to the GMP-IMERG.

is insignificant. For the semiarid region, the finer resolution model shows slightly better performance in FAR (Figure 6k). The 27 km resolution performs better than others in terms of POD and CSI when the KF CP scheme is used. The 9 km resolution model performs reasonably well with BMJ and GF CP schemes showing a modest improvement over the 27 km resolution.

In terms of MBE, the finer resolution model shows a mostly negative bias, while the coarser resolutions are positive (Figures 7a–7c). In the heavy rainy area, the performance of the 3 km resolution is better in terms

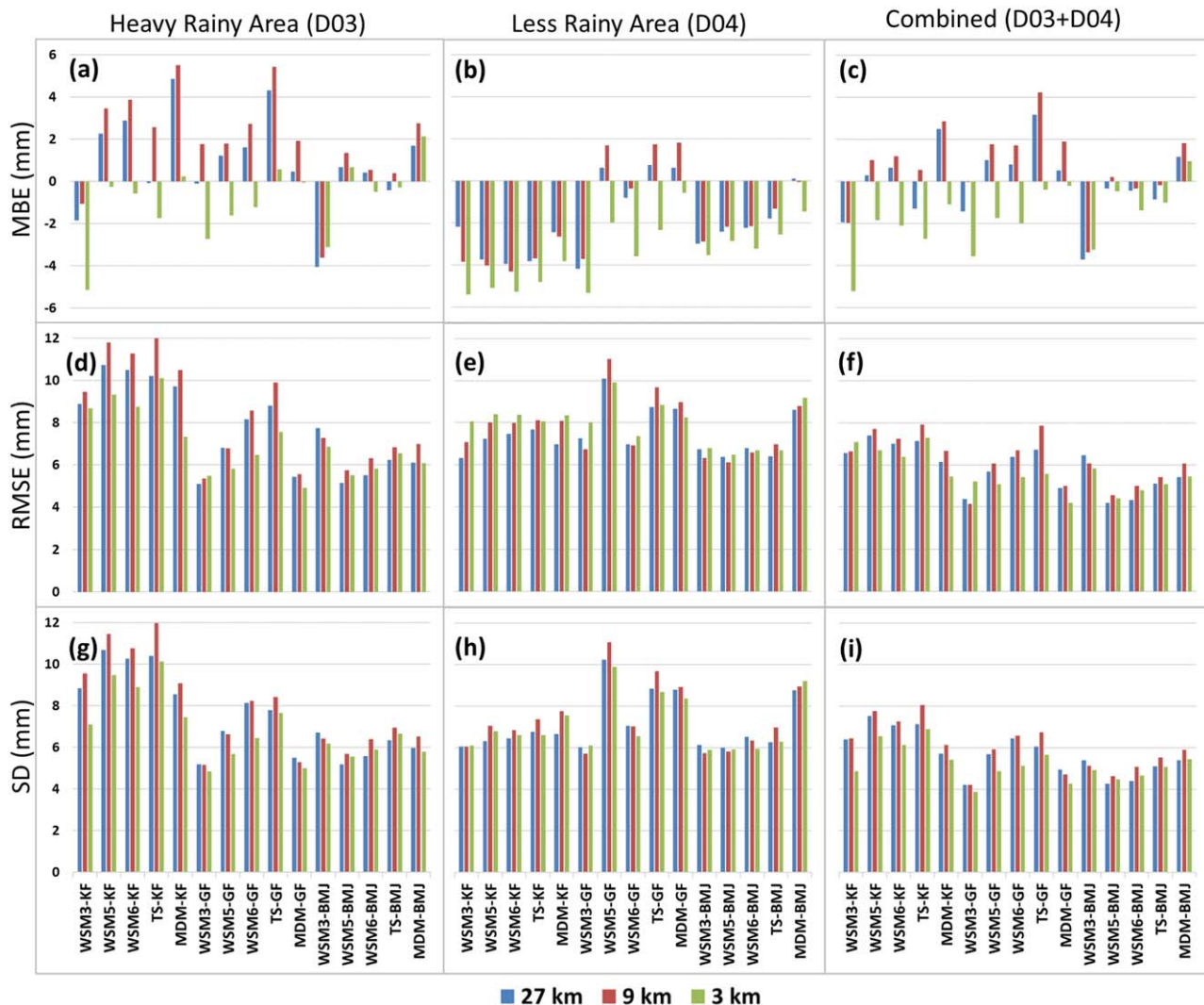


Figure 7. Same as Figure 6 but in terms of accuracy in areal-averaged precipitation with respect to the NCDC-GSOD data.

of areal-averaged precipitation according to RMSE and SD metrics (Figures 7d and 7g). In the less rainy (semiarid) area, the sensitivity to spatial resolution is insignificant in terms of RMSE and SD metrics (Figures 7e and 7h). In TOPSIS RCV plots (Figure 8), the overall performance of the finer resolution model is not significantly higher than with coarser resolution, except for the case of TS and MDM MP schemes in the combined case (Figure 8c). The MDM is the most sophisticated MP scheme used in this study with a total of 10 variables [Rajeevan *et al.*, 2010]. The TS is the second most complex MP scheme used here. In general, the higher resolution model demands a complex microphysics scheme (*i.e.*, with more variable) to resolve finer-scale processes explicitly [Stensrud, 2007]. This indicates the necessity of a complex MP scheme in high resolution to resolve convective process explicitly when no cumulus physics are used. This may explain why the performance of the 3 km resolution is remarkably better than the coarse resolution model with the TS and MDM MP schemes.

The CP scheme was not used with 3 km resolution in this study. The WSM3-GF combination was chosen to assess the performance of the 3 km resolution model using the CP scheme, as this combination shows good performance for 27 km and 9 km resolutions, but remarkably poor performance at 3 km resolutions (Figure 8c). We used the unified score (equation (1)) to compare the results before and after using the CP scheme in the 3 km resolution. The simulation of 3 km resolution with the CP scheme significantly improves model performance in finer resolution in terms of unified score (Figure 9). A possible reason could be that the relatively simple WSM3-MP scheme (with only three variables) is unable to capture the convective

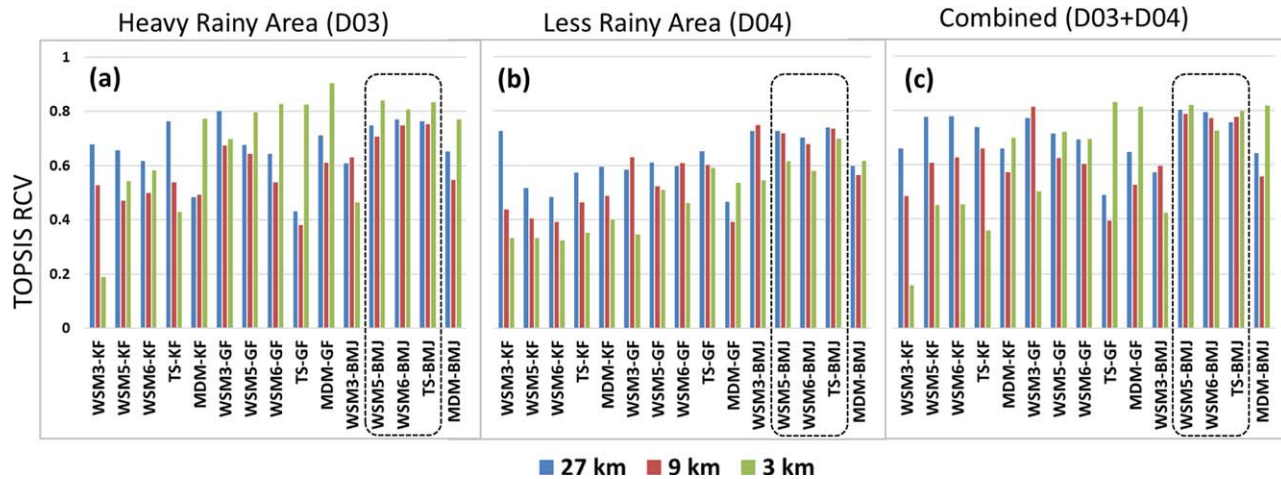


Figure 8. Topsis RCV of different combinations (MP-CP and spatial resolution) in GBM basins for the 2015 monsoon season. Higher Topsis RCV means it is more optimal. The selected combinations (i.e., with better and consistent performance) are shown by dashed border.

process in the finer resolution grids. Use of the CP scheme appears to overcome this limitation. Therefore, additional care may be required for the higher-resolution WRF model simulations, where convective precipitation is common. The higher-resolution model performance can be improved by using the CP scheme with it or by using any sophisticated MP scheme with many variables when no CP scheme is used.

Figure 10 shows areal-averaged precipitation for all three likely best MP-CP combinations in conjunction with the observed data (GSOD) at different spatial resolutions for all domains (wet, dry, and combined). In the heavy rainy area, the WRF model is able to capture the 20 and 30 August storm events that took place in GBM (GSOD in Figures 10a/10d/10g). All model combinations are found to overestimate the first storm event and underestimate the second storm event. The 27 km resolution shows relatively better performance in the first storm event using the WSM6 scheme (Figure 10a), while the 9 km resolution with WSM5 is best for the second event (Figure 10d). In the less rainy (semiarid) area, all model combinations show poor performance and fail to capture the storm events on 11 August, but are able to capture the 17 August storm event (Figure 10b, 10e, and 10h). In general, the use of 3 km resolution does not yield superior skill in terms of areal-averaged precipitation. Finally, the difference between the Topsis RCV of the 27 km and 9 km resolutions is less than the difference with the 3 km resolution in the combined case (Figure 8c). Therefore, both 27 km and 9 km resolutions can be considered to be part of the likely ideal set of combinations.

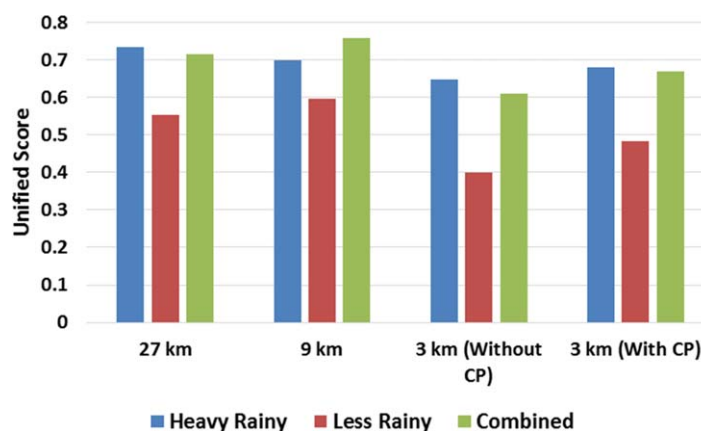


Figure 9. Comparison between the unified scores of the WSM3-GF combination in higher resolution (3 km) using CP and without CP in GBM basins for the 2015 monsoon season.

6.3. Reproducibility Over Indus Basin

The WRF model was set up over the Indus river basin using a set of three likely ideal MP-CP combinations and two resolutions identified over the GBM domain. The simulation period spanned a week time period when a severe storm event in late July 2010 took place and flooded large parts of Pakistan [Ahसान and Khan, 2013]. The peak of the storm occurred on 29 July 2010. Similar to the GBM basin, the accuracy of simulated precipitation was calculated using a

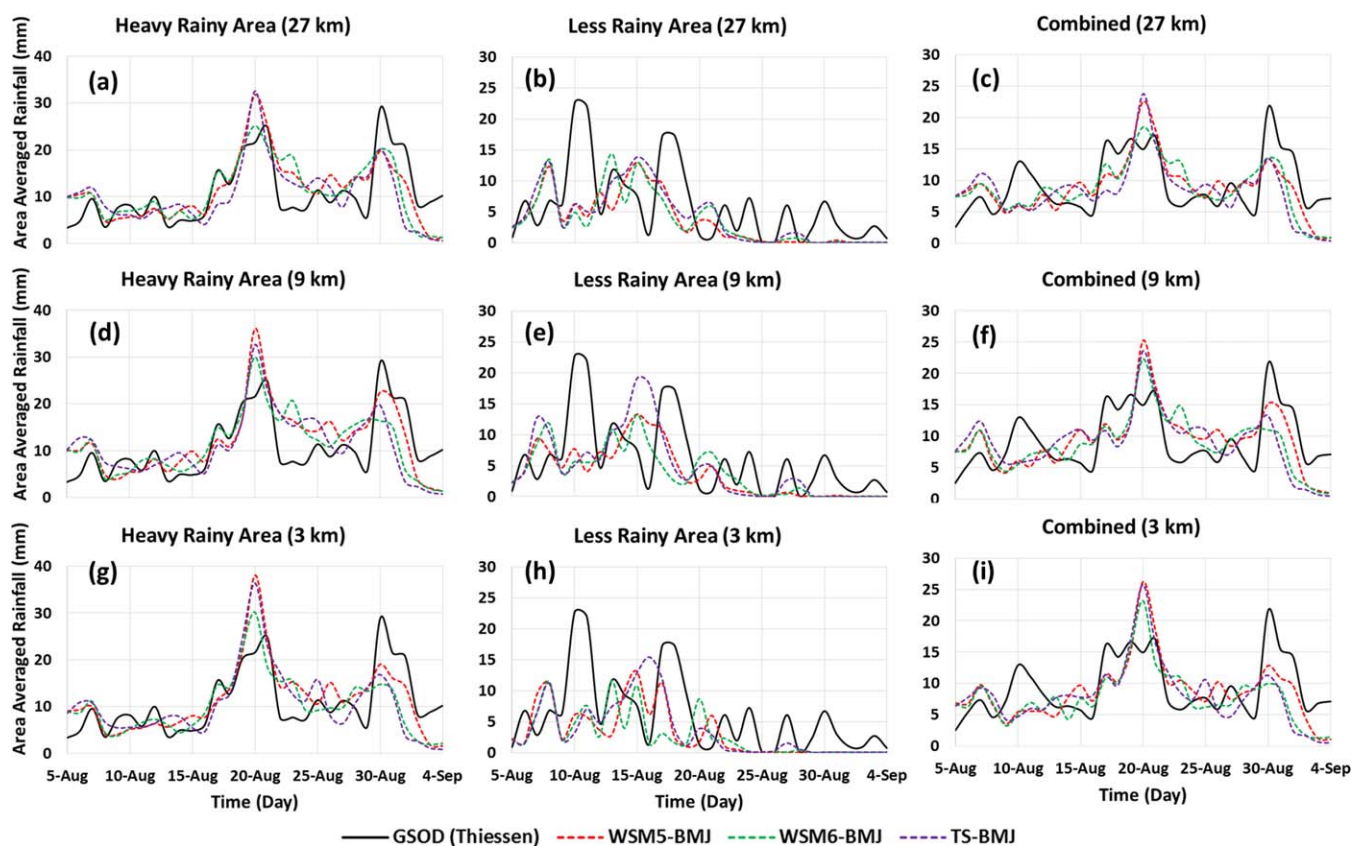


Figure 10. Comparison between areal-averaged precipitation for the three likely best MP-CP combinations and observed precipitation (GSOD) in GBM basins for the 2015 monsoon season. The extent of the heavy rainy areas and less rainy areas are shown in Figure 5. Combined areas consider both heavy and less rainy areas.

similar set of metrics (Figure 11). The CHIRPS data set was used as the reference data set to calculate the categorical metrics, as the GPM-IMERG data record only starts in 2014.

From Figure 11, it is visible that the difference among the three likely best sets of combinations (derived from GBM) in the Indus basin is marginal. Only the MBE shows that the TS-BMJ combination overestimates precipitation slightly more than the others. The unified score was calculated using equation (1) and compared with the unified score of GBM basins (Figure 12). The comparison shows that in both cases, the unified score yielded by the WSM5-BMJ is superior followed by the WSM6-BMJ and TS-BMJ combinations. In both basins, the 27 km resolution with WSM5-BMJ and WSM6-BMJ show slightly improved performance over the 9 km resolution. This indicates that the likely best combination of parameterizations hold true for the Indus basin and the yield skill is consistent to that observed for GBM basins (Figure 12).

The areal-averaged precipitation calculated for different likely best MP-CP combinations and resolutions are shown in Figure 13 along with the observed data. The storm was captured by all combinations, but appeared to have an offset in the time to peak. WRF estimated the timing when rainfall peaked by about a day. The peak achieved by the TS-BMJ combination was somewhat closer to the observed (Figure 13). Performance of the other combinations is similar as reflected in the unified score values (Figure 12).

Overall, our sensitivity analyses indicate that the WSM5-BMJ at 27 km resolution shows the ideal performance for both GBM and Indus river basins. This therefore serves as a tremendously useful guide and starting platform for various flood forecasting agencies around the world that deal with monsoon-driven seasonal flooding. The validation and reproducibility of performance on an independent and neighboring basin (Indus) to GBM indicates that findings are representative of the broader South Asian Monsoon climate. For assessing robustness beyond South Asia, further analyses in farther away Monsoon-affected basins such as the Mekong or Upper Nile are required.

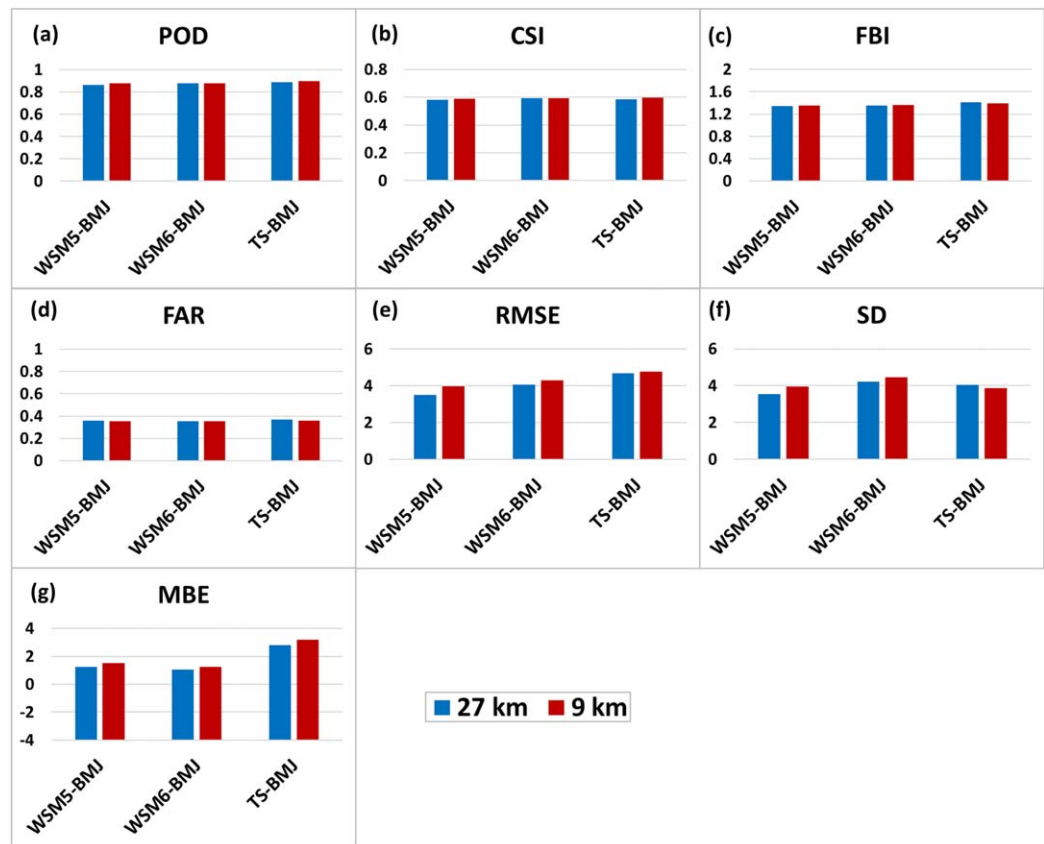


Figure 11. Comparison between the performance of the likely best MP-CP and spatial resolution combinations in the Indus basin for a one week time period for the late July 2010 storm event. The most optimized value for POD, CSI, and FBI is 1 and is 0 for FAR, RMSE, SD, and MBE.

6.4. Assessment of Forecast Skill

The previous analyses used WRF nowcast (or in other words—retrospective simulation based on boundary conditions from the NCEP GFS final analysis). In this section, we show the performance of the likely best set of combinations in forecast mode using GFS forecast boundary condition data (GFS real-time forecast from NCEP). For computational efficiency, two storm events were selected that occurred on 20 and 30 August 2015 in the heavy rainy area of the GBM basins. The areal-averaged precipitation of two storms at lead times up to 10 days along with the observed data (GSOD) are shown in the top plot of Figure 14. The comparison shows that the WRF model configuration is able to downscale and maintain skill of the GFS forecast

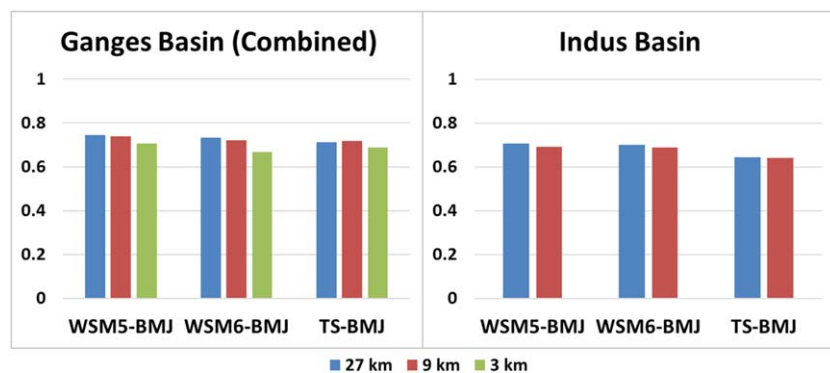


Figure 12. Comparison between the performances of the likely best MP-CP combinations in GBM basins for the 2015 monsoon season (one month) and Indus basin for the storm event of late July 2010 (1 week) in terms of unified score.

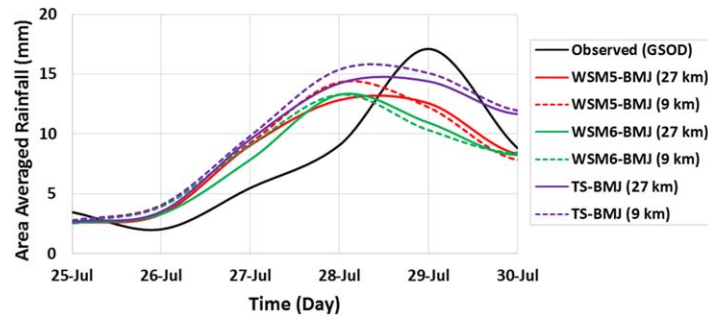


Figure 13. Same as Figure 10 but in the Indus basin domain for the storm event of late July 2010.

well enough to capture the first storm event (20 August). The 9 km resolution shows better performance than 27 km resolution across all combinations after the 5 day lead time. We believe, the “rising trend” in skill between lead times ranging from 5 to 7 days should not be given too much consideration at this stage given that only two events were studied in a limited manner. Rather, what is more telling from Figure 14 is

that the 30 August 2015 storm could not be forecast well using any of the WRF combinations. Another point to note is that for the 20 August storm, the WSM6-BMJ combination performs similar to the WSM5-BMJ combination (Figure 14 bottom plot).

We should note here that the time period selected, especially for assessment of forecast skill, is quite short (a week) compared to what would have been normally desirable. Our main limitation was CPU resources because running WRF in 45 different configurations and scales for an extended period was a logistic challenge. Nevertheless, readers should note the 1 week assessment as a potential limitation to making broad-based conclusions for the global Monsoon system. For example, we were not able to study how forecasting performs during El Nino or La Nina years or other types of oscillations with such a short period. Rather, the findings should be considered strictly limited to an “average” South Asian monsoon wherein the precipitation characteristics are assumed to be relatively steady in time during the months of July–October.

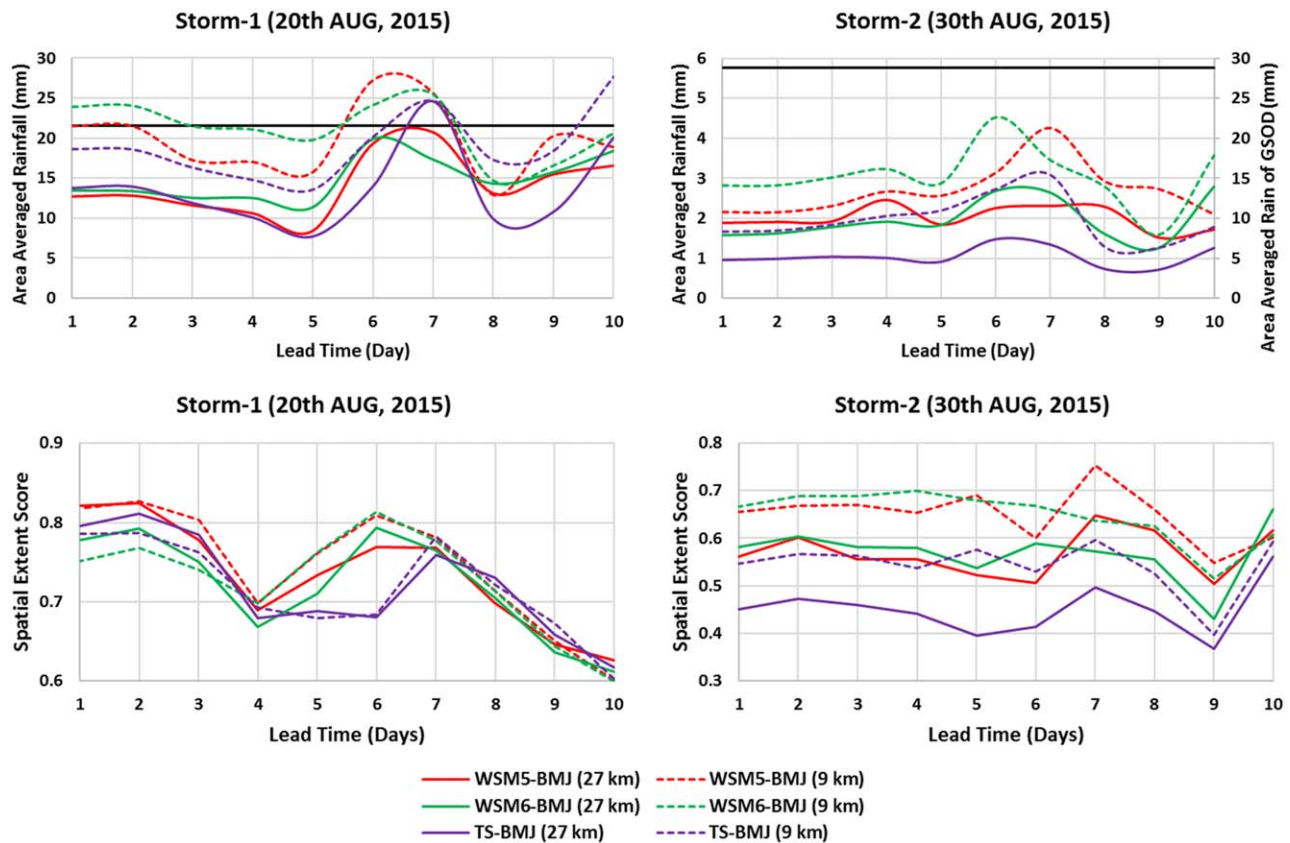


Figure 14. (top) Comparison of areal-averaged precipitation in forecast mode using the likely best MP-CP combinations along with the observed (GSOD in black line) as a function of lead times. (bottom) The skill of forecasted precipitation in terms of spatial distribution.

7. Conclusions

In this study, we explored the likely ideal set of WRF physics combination for simulating (downscaling) precipitation from a global NWP model over the monsoon-dominated region of the Ganges-Brahmaputra-Meghna river basins. The likely ideal combination was validated in a neighboring basin. Such an evaluation helped pinpoint a more manageable set of parameterizations for atmospheric modelers that may need further refinement through field campaigns for operational readiness in flood forecasting operations.

It was found that the Indian monsoon rainfall regime is more sensitive to the cumulus physics scheme than the cloud microphysics scheme. Our study showed that the performance of the MP and CP scheme in dry and wet areas of the GBM basins are considerably different. Model sensitivity to the CP scheme was different in both areas, but overall the Betts-Miller-Janjic scheme performed better. The performance of the most complex MP scheme of our study was better in the heavy rainy areas, while the same scheme showed poor results in the less rainy areas of the region. We also found that the finest resolution without using any cumulus physics option underestimated precipitation when a simple cloud microphysics scheme was used with far less variables. On the other hand, a more complex microphysics scheme with more variables yielded better performance at the finest resolution without the use of cumulus physics parameterization. From a set of 15 combinations of WRF parameterizations and three spatial resolutions, the sensitivity study converged to a set of three likely best MP-CP combinations and two spatial resolutions. Using a multicriteria decision analysis, it was found that the WRF Single Moment 3 Class, WRF Single Moment 6 Class, and Thompson microphysics schemes with Betts-Miller-Janjic cumulus parameterization scheme works well with 27 and 9 km spatial resolution for all conditions in the GBM basin.

The study found that the likely ideal configurations derived using the GBM domain also held true for the Indus domain. In both regions, the WSM5-BMJ yielded the best result, followed by WSM6-BMJ and TS-BMJ combinations. The difference in performance between 27 and 9 km was marginal, indicating that computational efficiency could be achieved at 27 km without compromising accuracy. Additionally, the study tested the WRF precipitation simulation in forecast mode using GFS forecast boundary data for two storm events in the GBM basin. The results of this skill assessment yielded a mixed bag of results, where skill was found to be storm event sensitive. Although good forecast skill was achieved for a storm event on 20 August 2015, our study points to the need for more investigation in the forecast mode as a function of storm physics characteristics and quality of boundary condition data.

There is no doubt that flood forecasting with longer lead times along with sufficient accuracy can reduce the flood hazard in flood-prone countries. The only way to increase the lead time of a flood forecasting system beyond the hydrologic time of concentration is to produce accurate precipitation forecasts. We believe the freely available global NWP products and regional NWP model packages (like WRF) are the best tools to forecast precipitation in ungauged river basins by flood management agencies constrained by limited financial resources. Therefore, further development of modeling systems that downscale NWP model forecast should be explored for eventual use by operational flood forecasting agencies. Additional numerical models should also be considered, such as Regional Atmospheric Modeling System (RAMS) [e.g., Freitas *et al.*, 2016]. Use of additional numerical models allows a more robust assessment of forecast skill through multimodel ensembles. Future studies should include the following topics: (1) exploring further refinements to our proposed likely best set of parameterization configurations; (2) evaluation of model performance using forecasted boundary data from NWP models other than NOAA models; (3) exploration of multiple storm events of contrasting characteristics in different regions; (4) assimilation of satellite observations of the atmosphere to improve skill in precipitation forecasts; and (5) exploration of multimodel ensembles.

References

- Ahasan, M. N., and A. Q. Khan (2013), Simulation of a flood producing rainfall event of 29 July 2010 over north-west Pakistan using WRF-ARW model, *Nat. Hazards*, *69*(1), 351–363, doi:10.1007/s11069-013-0719-6.
- Assari, A., T. M. Maheshand, and E. Assari (2012), Role of public participation in sustainability of historical city: Usage of TOPSIS method, *Indian J. Sci. Technol.*, *5*(3), 2289–2294.
- Dudhia, J. (1989), Numerical study of convection observed during the Winter Monsoon Experiment using a mesoscale two-dimensional model, *J. Atmos. Sci.*, *46*(20), 3077–3107, doi:10.1175/1520-0469(1989)046<3077:NSOCOD>2.0.CO;2.
- Ebert, E. E. (2001), Ability of a poor man's ensemble to predict the probability and distribution of precipitation, *Mon. Weather Rev.*, *129*, 2461–2480.

Acknowledgments

This study was supported by NASA SERVIR grant (NNX12AM85G), NASA WATER grant (NNX15AC63G), and NSF Belmont Grand Challenge grant (NSF 1433501) awarded to the authors. Generous support from the University of Washington startup fund awarded to the second author and the Ivanhoe Foundation to the first author is also acknowledged. Data used in this study can be obtained from the following sources: (1) Model boundary data, NCEP GFS FNL (i.e., nowcast): <http://rda.ucar.edu/datasets/ds083.2/>; GFS Forecast: http://nomads.ncdc.noaa.gov/data.php#hires_weather_datasets; (2) Satellite precipitation data, GPM-IMERG: <http://pmm.nasa.gov/data-access/downloads/gpm>; CHIRPS: <ftp://chg-ftpout.geog.ucsb.edu/pub/org/chg/products/CHIRPS-2.0/>; and (3) Station-based precipitation data, NCDC-GSOD: <ftp://ftp.ncdc.noaa.gov/pub/data/gsod/>; The WRF model used was version WRF-ARW V3.7.1 and is available from http://www2.mmm.ucar.edu/wrf/users/download/get_source.html. All model output results are available upon request.

- Efstathiou, G. A., N. M. Zoumakis, D. Melas, C. J. Lolis, and P. Kassomenos (2013), Sensitivity of WRF to boundary layer parameterizations in simulating a heavy rainfall event using different microphysics schemes. Effect on large-scale processes, *Atmos. Res.*, *132*–133, 125–143.
- Flood Forecasting and Warning Centre (FFWC) (2014), Annual Flood Report 2014, Bangladesh Water Development Board, Dhaka. [Available at <http://www.ffwc.gov.bd/images/annual14.pdf>.]
- Freitas, S. R., et al. (2016), The Brazilian developments on the Regional Atmospheric Modeling System (BRAMS 5.2): An integrated environmental model tuned for tropical areas, *Geosci. Model Dev. Discuss.*, doi:10.5194/gmd-2016-130, in press.
- Funk, C., et al. (2015), The climate hazards infrared precipitation with stations—a new environmental record for monitoring extremes, *Sci. Data*, *2*, 150066, doi:10.1038/sdata.2015.66 2015.
- Georgakakos, K. P., N. E. Graham, T. M. Modrick, M. J. Murphy Jr., E. Shamir, C. R. Spencer, and J. A. Sperflage (2014), Evaluation of real-time hydrometeorological ensemble prediction on hydrologic scales in Northern California, *J. Hydrol.*, *519*, 2978–3000.
- Givati, A., B. Lynn, Y. Liu, and A. Rimmer (2012), Using the WRF Model in an Operational Streamflow Forecast System for the Jordan River, *J. Appl. Meteorol. Climatol.*, *51*, 285–299.
- Grell, G. A., and S. R. Freitas (2014), A scale and aerosol aware stochastic convective parameterization for weather and air quality modeling, *Atmos. Chem. Phys.*, *14*, 5233–5250, doi:10.5194/acp-14-5233-2014.
- Hong, S. Y., and J. O. J. Lim (2006), The WRF Single-Moment 6-Class Microphysics Scheme (WSM6), *J. Korean Meteorol. Soc.*, *42*(2), 129–151.
- Hong, S. Y., J. Dudhia, and S. H. Chen (2004), A revised approach to ice microphysical processes for the bulk parameterization of clouds and precipitation, *Mon. Weather Rev.*, *132*, 103–120, doi:10.1175/1520-0493(2004)132<0103:ARATIM>2.0.CO;2.
- Hong, S. Y., Y. Noh, and J. Dudhia (2006), A new vertical diffusion package with an explicit treatment of entrainment processes, *Mon. Weather Rev.*, *134*, 2318–2341, doi:10.1175/MWR3199.1.
- Hopson, T. M., and P. J. Webster (2010), A 1–10-day ensemble forecasting scheme for the major river basins of Bangladesh: Forecasting severe floods of 2003–07, *J. Hydrometeorol.*, *11*, 618–641.
- Hossain, F., and N. Katiyar (2006), Improving flood forecasting in international river basins, *EOS AGU*, *87*(5), 49–60.
- Hossain, F., N. Katiyar, Y. Hong, and A. Wolf (2007), The emerging role of satellite rainfall data in improving the hydro-political situation of flood monitoring in the under-developed regions of the world, *Nat. Hazards*, *43*(2), 199–210.
- Hsiao, L. F., et al. (2013), Ensemble forecasting of typhoon rainfall and floods over a mountainous watershed in Taiwan, *J. Hydrol.*, *506*, 55–68.
- Huffman, G. J., D. T. Bolvin, D. Braithwaite, K. Hsu, R. Joyce, and P. Xie (2015), GPM Integrated Multi-Satellite Retrievals for GPM (IMERG) Algorithm Theoretical Basis Document (ATBD) v4.5. [Available at http://pmm.nasa.gov/sites/default/files/document_files/IMERG_ATBD_V4.5_0.pdf.]
- Hwang, C. L., and K. Yoon (1981), *Multiple Attribute Decision Making: Methods and Applications*, Springer, Berlin.
- Jang, J., and S. Y. Hong (2014), Quantitative forecast experiment of a heavy rainfall event over Korea in a global model: Horizontal resolution versus lead time issues, *Meteorol. Atmos. Phys.*, *124*(3), 113–127.
- Janjic, Z. I. (1994), The Step–Mountain Eta Coordinate Model: Further developments of the convection, viscous sublayer, and turbulence closure schemes, *Mon. Weather Rev.*, *122*, 927–945, doi:10.1175/1520-0493(1994)122<0927:TSMCECM>2.0.CO;2.
- Jasper, K., J. Gurtz, and H. Lang (2002), Advanced flood forecasting in Alpine watersheds by coupling meteorological observations and forecasts with a distributed hydrological model, *J. Hydrol.*, *267*, 40–52.
- Kain, J. S. (2004), The Kain–Fritsch convective parameterization: An update, *J. Appl. Meteorol. Climatol.*, *43*, 170–181, doi:10.1175/1520-0450(2004)043<0170:TKCPAU>2.0.CO;2.
- Khromov, S. P. (1957), Die Geographische Verbreitung der Monsune, *Petermanns Geogr. Mitt.*, *101*, 234–237.
- Kumar, R. A., J. Dudhia, and S. K. R. Bhowmik (2010), Evaluation of Physics options of the Weather Research and Forecasting (WRF) Model to simulate high impact heavy rainfall events over Indian Monsoon region, *Geofizika*, *27*(2), 101–125.
- Kumar, P., M. V. Shukla, P. K. Thapliyal, J. H. Bisht, and P. K. Pal (2012), Evaluation of upper tropospheric humidity from NCEP analysis and WRF Model Forecast with Kalpana observation during Indian summer monsoon 2010, *Meteorol. Appl.*, *19*, 152–160, doi:10.1002/met.1332.
- Kumar, P., C. M. Kishitawal, and P. K. Pal (2016), Skill of regional and global model forecast over Indian region, *Theor. Appl. Climatol.*, *123*(3), 629–636, doi:10.1007/s00704-014-1361-2.
- Liguori, S., M. A. R. Ramirez, A. N. A. Schellart, and A. J. Saul (2012), Using probabilistic radar rainfall nowcasts and NWP forecasts for flow prediction in urban catchments, *Atmos. Res.*, *103*, 80–95.
- Liu, J., M. Bray, and D. Han (2012), Sensitivity of the Weather Research and Forecasting (WRF) model to downscaling ratios and storm types in rainfall simulation, *Hydrol. Processes*, *26*, 3012–3031.
- Liu, J., J. Wang, S. Pan, K. Tang, C. Li, and D. Han (2015), A real-time flood forecasting system with dual updating of the NWP rainfall and the river flow, *Nat. Hazards*, *77*, 1161–1181.
- Lowrey, M. R. K., and Z. Yang (2008), Assessing the capability of a regional-scale weather model to simulate extreme precipitation patterns and flooding in central Texas, *Weather Forecast.*, *23*(6), 1102–1126.
- Mannan, M. A., M. A. M. Chowdhury, and S. Karmakar (2013), Application of NWP model in prediction of heavy rainfall in Bangladesh, *Procedia Eng.*, *53*, 667–675.
- Milani, A. S., A. Shanian, R. Madoliat, and J. A. Nemes (2005), The effect of normalization norms in multiple attribute decision making models: A case study in gear material selection, *Struct. Multidiscip. Optim.*, *29*, 312–318, doi:10.1007/s00158-004-0473-1.
- Mirza, M. Q., R. A. Warrick, N. J. Erickson, and G. J. Kenny (1998), Trends and persistence in precipitation in the Ganges, Brahmaputra and Meghna river basins, *Hydrol. Sci. J.*, *43*(6), 845–858.
- Mlawer, E. J., S. J. Taubman, P. D. Brown, M. J. Iacono, and S. A. Clough (1997), Radiative transfer for inhomogeneous atmospheres: RRTM, a validated correlated- k model for the longwave, *J. Geophys. Res.*, *102*(D14), 16,663–16,682, doi:10.1029/97JD00237.
- Morrison, H., and G. Thompson (2009), Impact of cloud microphysics on the development of trailing stratiform precipitation in a simulated squall line: Comparison of one– and two–moment schemes, *Mon. Weather Rev.*, *132*, 103–120, doi:10.1175/2008MWR2556.1.
- Mukhopadhyay, P., S. Taraphdar, B. N. Goswami, and K. Krishnakumar (2010), Indian summer monsoon precipitation climatology in a high-resolution regional climate model: Impacts of convective parameterization on systematic biases, *Weather Forecast.*, *25*(2), 369–387, doi:10.1175/2009WAF2222320.1.
- Nam, D. H., D. T. Mai, K. Udo, and A. Mano (2014), Short-term flood inundation prediction using hydrologic-hydraulic models forced with downscaled rainfall from global NWP, *Hydrol. Processes*, *28*, 5844–5859.
- Pennelly, C., G. Reuter, and T. Flesch (2014), Verification of the WRF model for simulating heavy precipitation in Alberta, *Atmos. Res.*, *135*–136, 172–192.
- Rajeevan, M., A. Kesarkar, S. B. Thampi, T. N. Rao, B. Radhakrishna, and M. Rajasekhar (2010), Sensitivity of WRF cloud microphysics to simulations of a severe thunderstorm event over Southeast India, *Ann. Geophys.*, *28*, 603–619.

- Ramage, C. S. (1971), *Monsoon Meteorology*, Academic, London, U. K.
- Rao, Y. V. R., H. R. Hatwar, A. K. Salah, and Y. Sudhakar (2007), An experiment using the high resolution Eta and WRF models to forecast heavy precipitation over India, *Pure Appl. Geophys.*, *164*, 1593–1615.
- Roberts, N. M., S. J. Cole, R. M. Forbes, R. J. Moore, and D. Boswell (2009), Use of high-resolution NWP rainfall and river flow forecasts for advance warning of the Carlisle flood, north-west England, *Meteorol. Appl.*, *16*, 23–34.
- Skamarock, W. C., J. B. Klemp, J. Dudhia, D. O. Gill, D. M. Barker, M. G. Duda, X. Y. Hung, W. Wang, and J. G. Powers (2008), A description of the advanced research WRF Version 3, *NCAR Tech. Note NCAR/TN-475+STR*, Nat. Cent. Atmos. Res., Boulder, Colo.
- Srinivas, C. V., D. Hariprasad, D. V. B. Rao, Y. Anjaneyulu, R. Baskaran, and B. Venkatraman (2013), Simulation of the Indian summer monsoon regional climate using advanced research WRF model, *Int. J. Climatol.*, *33*(5), 1195–1210, doi:10.1002/joc.3505.
- Srinivas, C. V., D. H. Prasad, D. V. B. Rao, R. Baskaran, and B. Venkatraman (2015), Simulation of the Indian summer monsoon onset-phase rainfall using a regional model, *Ann. Geophys.*, *33*(9), 1097–1115.
- Stensrud, D. J. (2007), *Parameterization Schemes: Keys to Understanding Numerical Weather Prediction Models*, Cambridge Univ. Press, Cambridge.
- Tewari, M., F. Chen, W. Wang, J. Dudhia, M. A. LeMone, K. Mitchell, M. Ek, G. Gayno, J. Wegiel, and R. H. Cuenca (2004), Implementation and verification of the unified NOAA land surface model in the WRF model, in *20th Conference on Weather Analysis and Forecasting/16th Conference on Numerical Weather Prediction*, Amer. Meteorol. Soc., Seattle, Wash.
- Thompson, G., P. R. Field, R. M. Rasmussen, and W. D. Hall (2008), Explicit forecasts of winter precipitation using an improved bulk microphysics scheme. Part II: Implementation of a new snow parameterization, *Mon. Weather Rev.*, *136*, 5095–5115, doi:10.1175/2008MWR2387.1.
- Ulate, M., J. Dudhia, and C. Zhang (2014), Sensitivity of the water cycle over the Indian Ocean and Maritime Continent to parameterized physics in a regional model, *J. Adv. Model. Earth Syst.*, *6*, 1095–1120, doi:10.1002/2014MS000313.
- UN-Water (2008), *Transboundary Waters: Sharing Benefits, Sharing Responsibilities*, Thematic Paper, UN-Water, Zaragoza, Spain. [Available at http://www.unwater.org/downloads/UNW_TRANSBOUNDARY.pdf.]
- Upadhyaya, S., and R. Ramsankaran (2014), Multi-index rain detection: A new approach for regional rain area detection from remotely sensed data, *J. Hydrometeorol.*, *15*, 2314–2330, doi:10.1175/JHM-D-14-0006.1.
- Vaidya, S. S. (2006), The performance of two convective parameterization schemes in a mesoscale model over the Indian region, *Meteorol. Atmos. Phys.*, *92*(3), 175–190.
- Verbunt, M., M. Zappa, J. Gurtz and P. Kaufmann (2006), Verification of a coupled hydrometeorological modelling approach for alpine tributaries in the Rhine basin, *J. Hydrol.*, *324*, 224–238.
- Yucel, I., and A. Onen (2014), Evaluation a mesoscale atmosphere model and a satellite-based algorithm in estimating extreme rainfall events in northwestern Turkey, *Nat. Hazards Earth Syst. Sci.*, *14*, 611–624.
- Yucel, I., A. Onen, K. K. Yilmaz, and D. J. Gochis (2015), Calibration and evaluation of a flood forecasting system: Utility of numerical weather prediction model, data assimilation and satellite-based rainfall, *J. Hydrol.*, *523*, 49–66.
- Zhang, D., and R. A. Anthes (1982), A high-resolution model of the planetary boundary layer— sensitivity tests and comparisons with SESA-ME-79 data, *J. Appl. Meteorol. Climatol.*, *21*, 1594–1609, doi:10.1175/1520-0450(1982)021 < 1594:AHMOT > 2.0.CO;2.
- Zheng, Y., K. Alapaty, J. A. Herwehe, A. D. D. Genio, and D. Niyogi (2016), Improving high-resolution weather forecasts using the Weather Research and Forecasting (WRF) model with an updated Kain-Fritsch scheme, *Mon. Weather Rev.*, *144*, 833–860, doi:10.1175/MWR-D-15-0005.1.